# TRITON
# Algorithm Theoretical Basis Document v1.0

**Taiwan Space Agency**

**國 家 太 空 中 心**

# TABLE OF CONTENTS

# 1 Introduction

This document provides a description of TRITON data process in different levels. The products of TRITON mission are in four levels, level 0, 1a, 1b, and 2. The data levels can be corresponding to the product generation flow which is shown in Figure 1-1. The ellipses in Figure 1-1 are the name of algorithm and the squares are the data or products. The red and purple ellipses are indicated for data processing or system management. The description of data in each level and the correspondence to product generation flow is in below.

## Level 0

The telemetry frames in Figure 1-1. The raw data down link from satellite. The format of Level 0 data is binary format and not be released.

## Level 1a

The l1aDdm in Figure 1-1. The information in level 1a data is the raw data down link from satellite recorded in netCDF format.

## Level 1b

The l1bDdm in Figure 1-1. The Level 1b CorDDM data is recorded in netCDF format and information in Level 1b CorDDM data is the same to level 1a and has been corrected the time shift occurs in receiver software. In Level 1b CorDDM data also record the calibrated DDM which remove the effect from the antenna and receiver.

The Supporting data in Figure 1-1. The Level 1b supporting data is recorded in netCDF format. The information in Level 1b metadata is the intermediate data calculated from Level 1b CorDDM data for further application. The main information in Level 1b metadata are the code phase and Doppler frequency of specular point (SP), effective scattering area, and normalized bistatic radar cross section (NBRCS) etc.

## Level 2

The U10 and roughness in Figure 1-1. The retrieved ocean surface wind speed (U10 < 20m/s) and roughness (mean square slope and significant height) are recorded in Level 2 data.

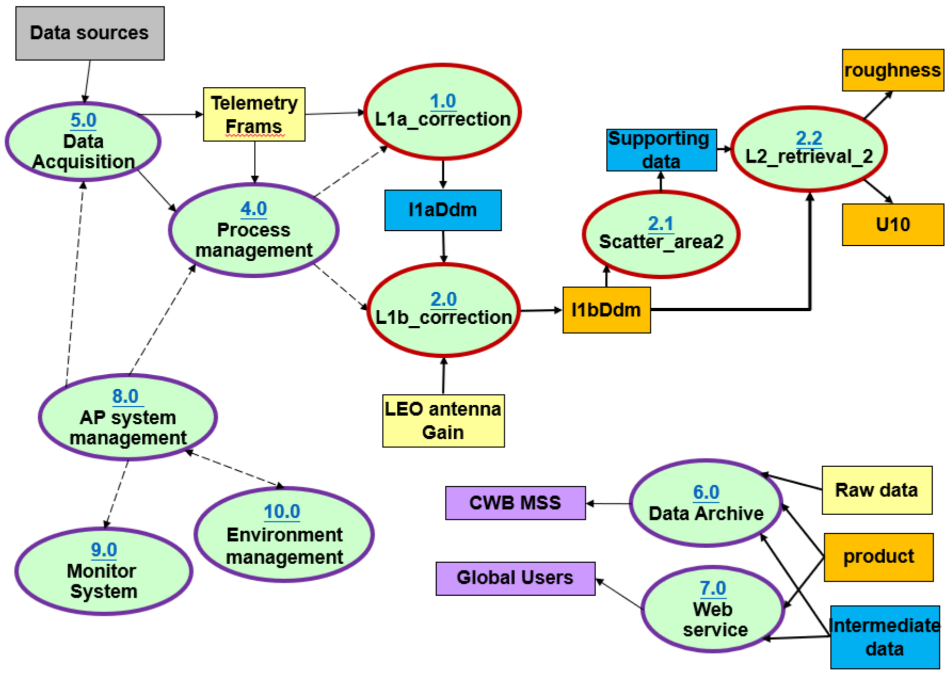


Figure 1-1 Product generation flow of TRITON mission.

## 2 Level 1a calibration

Due to the delay-Doppler map (DDM) is the signal strength of the received signal in different code phase delay and Doppler frequency, the signal strength is affected by the payload hardware. The level 1a calibration process is to derive the gain value of the payload to calculate the power of the received signal in different code phase delay and Doppler frequency.

The value of each bin in DDM can be described by

by

$$C = G(P_g + P_n + P_a + P_r), \quad (1)$$

where

$C$：the DDM values in counts
$G$ ： the total instrument gain applied to the incoming signal and noise in counts per watt
$P_a$：the thermal noise power received by the antenna in watts
$P_g$：the scattered signal power received by the instrument in watts
$P_r$：the thermal noise power generated by the instrument in watts

$P_n$：the noise power generated by the received signal with wrong PRN
$P_a$=k*$T_a$*$B_w$
$P_r$=k*$T_r$*$B_w$
k：Boltzmann’s constant=1.380649e-23

$T_a$ & $T_r$ : antenna and receiver temperature
$B_w$: signal bandwidth

The noise floor $C_n$ of DDM can be described by

$$C_n = G(P_n + P_a + P_r). \quad (2)$$

However, due to the $P_n$ of each DDM is different, it needs to be removed to calculate $G$ by

$$C_{min} = G(P_a + P_r), \quad (3)$$

then $P_g$ can be derived by

$$P_g = (C - C_n)\frac{(P_a + P_r)}{C_{min}}. \quad (4)$$

$C_{min}$ in (3) is derived by statistical method. Assume the relation between receiver and antenna temperature and noise floor is follow the equation

$$(noise\ floor, C_{min}) = a \times (antenna\ temperature) + b \times (receiver\ temperature) + c. \quad (5)$$

The process of $C_{min}$ is illustrated in Figure 2-1. The first step of the process is to get the minimum noise floor of different antenna and receiver temperature. Then remove the data with less sampling. The relation between data sampling and minimum noise floor is shown in the right bottom panel in Figure 2-1. In the right bottom panel of Figure 2-1, the minimum noise floor with less sampling, which are indicated in black, are higher than with more sampling and are removed before analysis. The noise floor with less sampling before and after removing are shown in left top and right top panels in Figure 2-1, respectively. The second step is to remove the data too dispersed from the mean value of minimum noise floor. The data too dispersed from the mean value of minimum noise floor are indicated in light blue. The remaining data after first and second step are indicated in dark blue. The third step is to regress the remaining data by using (5). The regress results are indicated in red in the right bottom panel and also shown in the left bottom panel in Figure 2-1. The third step is to regress the coefficient $a$ and b in (5). The coefficient c in (5) is calculated by using the noise floor measured from the payload when TRITON in the dormitory with fixed antenna and receiver temperature.

In second step, if the degree of dispersion for data removing is different, the regress result is also different. In order to determine the best coefficient of regression, eight different degree of dispersion is used for analysis. The DDM after corrected is used for DDM average (DDMA) calculation and then compare with the mean square slope (MSS), significant height (Hs), and ocean surface wind speed (OSWS). The comparisons are shown in Figure 2-2. The convergence degree is calculated by counting the number of samples located in the left bottom white area in Figure 2-2 and shown in Figure 2-3. In Figure 2-3, the convergence degree of case 4 to 8 are higher than case 1 to 3. Due to the long term variation of the coefficients in (5) of case 5 to 7 is much stable than case 4 and 8, the coefficients in (5) for correction are the mean value of case 5 to 7 by using 100 days data.

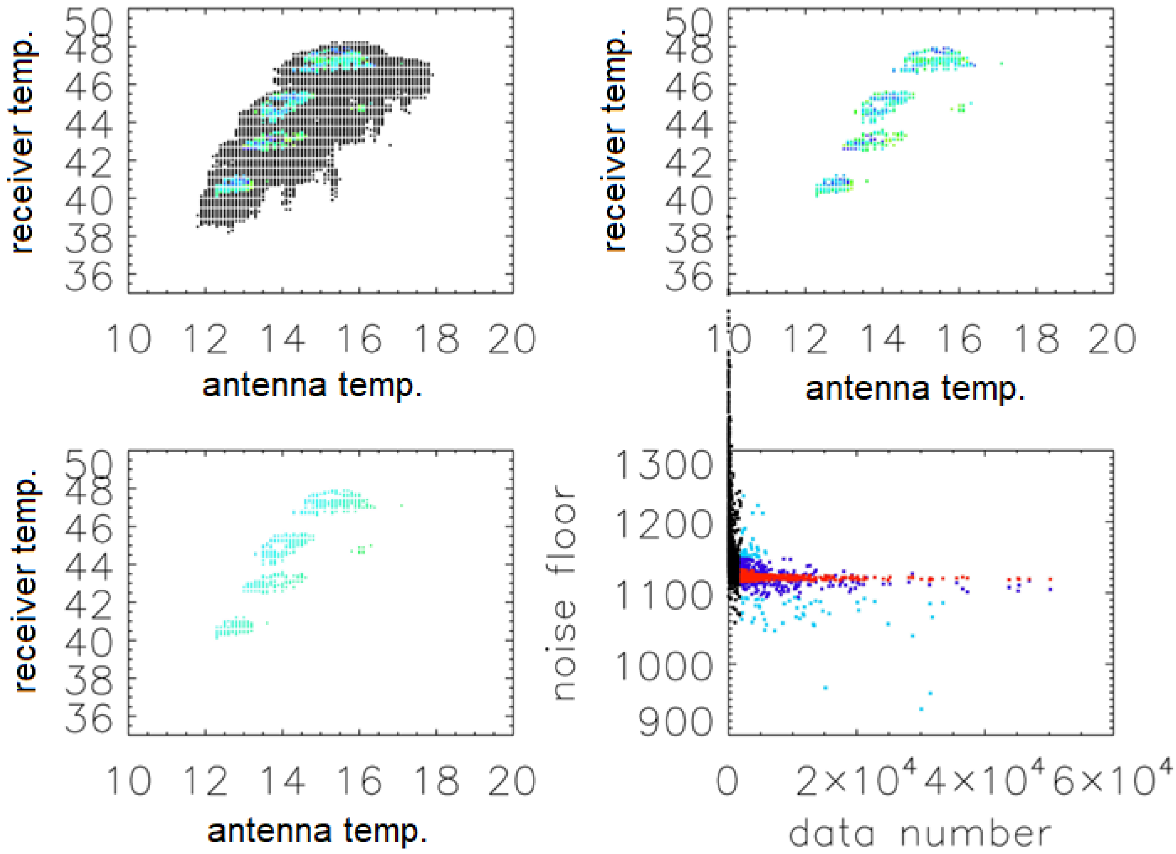


Figure 2-1 The illustration of $C_{min}$ derivation in (3). Left top：the minimum noise floor in different antenna and receiver temperature. The color indicates the level of noise floor and black indicates the data not put into deriving process；right top：the left top panel removes the black data；left bottom：the regression result of the data in right top panel；right bottom：the relation between data number and minimum noise floor. In right bottom panel, the black and light blue data are removed due to less sampling and too dispersed. The dark blue and red data are the data used for regression by (5) and the regression result.

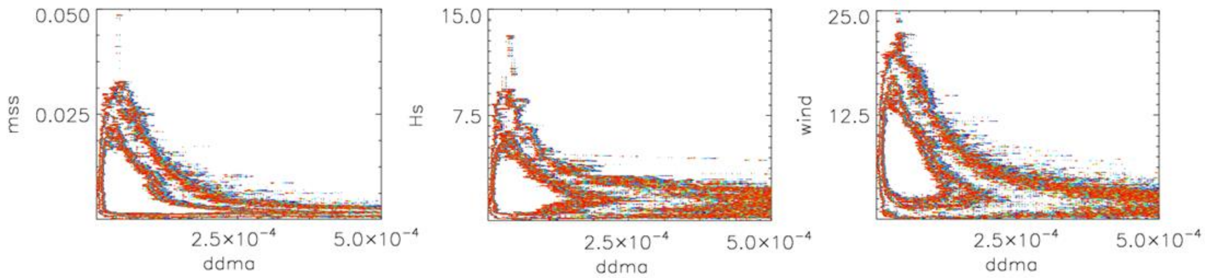


Figure 2-2 The comparison between DDMA calculated by corrected DDM with different degree of dispersion removing for regression. The different degree of dispersion is indicated in different color.

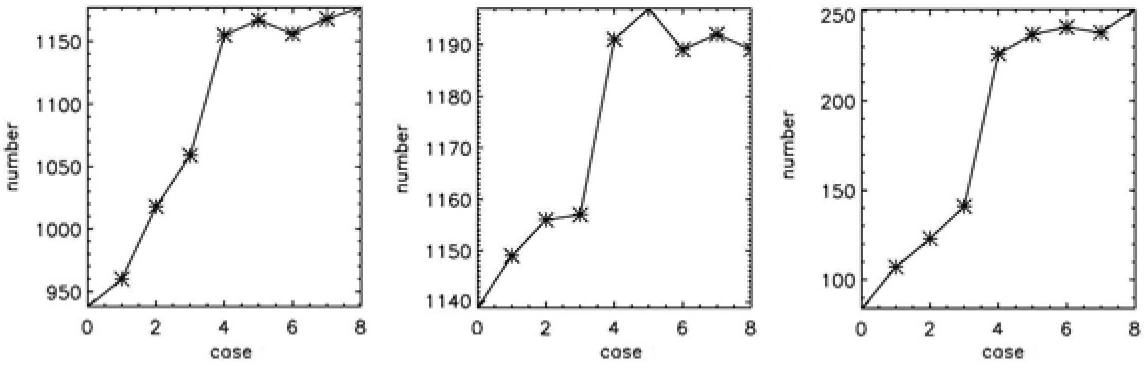


Figure 2-3 The DDMA convergence degree of eight different cases by comparing with MSS (left), Hs (middle), and wind speed (right).

# 3 Level 1b supporting data calculation

Level 1b supporting data provides the intermediate data calculated from level 1b data. The main intermediate data is the code phase delay and Doppler frequency of SP and the NBRCS. The code phase delay and Doppler frequency of SP is determinated by comparing the shape of DDM and effective scattering area (ESA). The shape of ESA can be calculated by using the position and velocity of TRITON and GPS satellite. After calculating ESA, the relative position of SP in ESA is confirmed. Then slide the shape of ESA in different code phase delay and Doppler frequency and find the best matching result between ESA and DDM. Four matching results between ESA and DDM are shown in the top four panels and the contour comparisons between ESA and DDM are shown in the bottom four panels of Figure 3-1. In the bottom four panels of Figure 3-1, the yellow and blue asterisks are indicated the position of SPs determined from ESA comparison and positions of TRITON and GPS satellites, respectively. The position of yellow asterisks for SP position is more reasonable.

The DDM theoretical model by Zavorotny and Voronovich (Z-V model) (Zavorotny and Voronovich, 2000) is

$$\langle P(\hat{\tau}, \hat{f}^D) \rangle = \frac{P^T \lambda^2}{(4\pi)^3} \iint_S \frac{G^T G^R}{R_0^2 R^2} \Lambda^2 (\frac{\delta\tau}{\tau_c}) S^2 (\frac{\delta f^D}{T_i}) \sigma_0 d^2 r \qquad (6)$$

where $P(\hat{\tau}, \hat{f}^D)$ is the scattered signal power with different code phase delay $\hat{\tau}$ and Doppler frequency $\hat{f}^D$. And $P^T$, $G^T$, $G^R$, $\delta\tau$, $\delta f^D$, $\tau_c$, $T_i$, $S$, $r$, $R$, $R_0$, $\Lambda^2(\ldots)S^2(\ldots)$, and $\sigma_0(r)$ are GPS satellite transmit power, GPS antenna gain at the specular point, receiver antenna gain at the specular point, the difference between the code phase delay of $r$ and $\hat{\tau}$, the difference between the Doppler frequency of $r$ and $\hat{f}^D$, chip, coherent integration time, the scattering surface, the point on the scattering surface, transmitter range from the scattering point, receiver range from the scattering point, WAF of pseudorandom C/A sequences, and normalized BRCS (NBRCS), respectively. (6) can be simplified as (CYGNSS, 2018)

$$\langle P(\hat{\tau}, \hat{f}^D)\rangle = \frac{P^T \lambda^2 G^T G^R \sigma_0 \bar{A}_{eff}}{(4\pi)^3 R_0^2 R^2} \tag{7}$$

where $\bar{A}_{eff}$ is effective scattering area. Then NBRCS can be written as

$$\sigma_0 = \langle P(\hat{\tau}, \hat{f}^D)\rangle \frac{(4\pi)^3 R_0^2 R^2}{P^T G^T \lambda^2 G^R \bar{A}_{eff}}. \tag{8}$$

Due to the GPS satellite transmit power and GPS antenna gain cannot obtain immediately, these two terms are not be removed and the provided NBRCS are calculated as

$$P^T G^T \sigma_0 = \langle P(\hat{\tau}, \hat{f}^D)\rangle \frac{(4\pi)^3 R_0^2 R^2}{\lambda^2 G^R \bar{A}_{eff}}. \tag{9}$$

The three NBRCS calculated by using three different bin number, $1 \times 1$, $3 \times 5$, and $13 \times 21$ with the SP bin located in center, are provided. The illustrations of three area with three different bin number in DDM and ESA are shown in Figure 3-2. The comparisons between three NBRCS by using around three months data are shown in Figure 3-3. In Figure 3-3, most of data are located near the blue line, which with slope equal to 1, and validated the accuracy of the SP code phase delay and Doppler frequency determination.

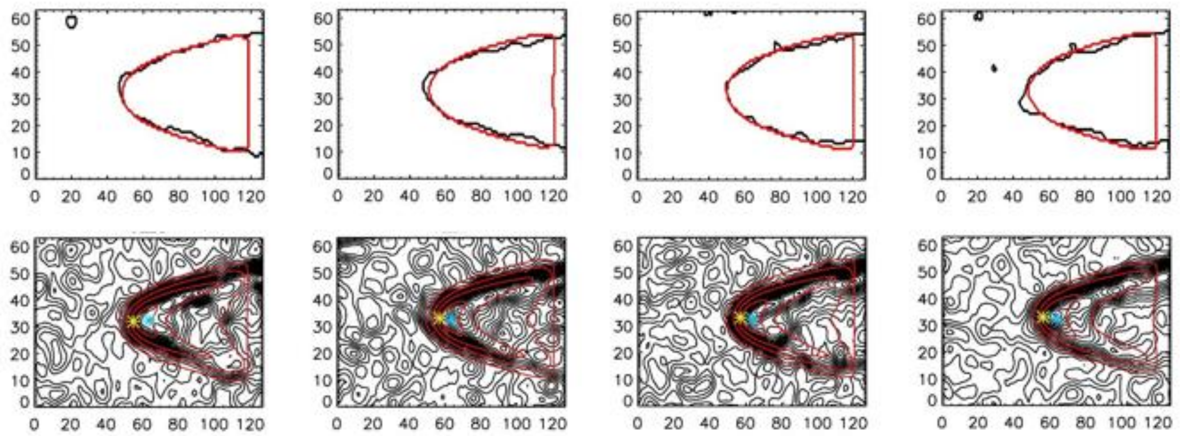

Figure 3-1 Top：Matching results between ESA and DDM. Bottom：Contour comparisons between ESA (red) and DDM (black). The yellow and blue asterisks are indicated the position of SPs determined from ESA comparison and positions of TRITON and GPS satellites, respectively.

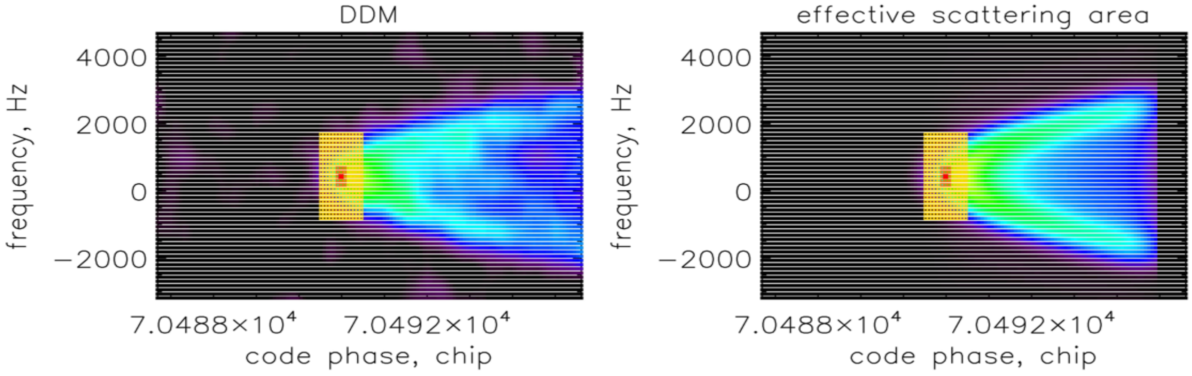


Figure 3-2 Illustration of three different bin number, $1 \times 1$, $3 \times 5$, and $13 \times 21$ with the SP bin located in center in DDM (left) and ESA (right). The area of $1 \times 1$, $3 \times 5$, and $13 \times 21$ are indicated by red dot, red rectangle, and yellow rectangle.

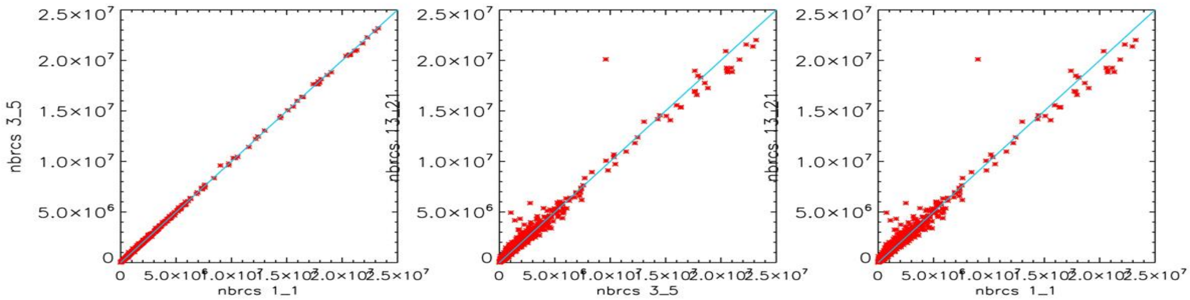


Figure 3-3 Comparisons between three NBRCS calculated by using three different number bins. The blue line in each panel is the line with slope equal to 1. (left) Comparison between NBRCS calculated by using $1 \times 1$ and $3 \times 5$ bins. (middle) (left) Comparison between NBRCS calculated by using $3 \times 5$ and $13 \times 21$ bins. (right) Comparison between NBRCS calculated by using $1 \times 1$ and $13 \times 21$ bins.

# 4 Level 2 products retrieving

TRITON satellite mission has three level 2 products, OSWS, MSS, and Hs.

The OSWS is retrieved by geophysical model function (GMF). The GMF for OSWS is derived from the comparison between DDMA and European Centre for Medium-Range Weather Forecasts (ECMWF) OSWS. The comparisons of DDMA with signal incident angle around 15 degree is shown in Figure 4-1. In the left and right panel of Figure 4-1 are the comparison between ECMWF OSWS and DDMA, and between DDMA and ECMWF OSWS, respectively, and the orange dots in the two panels are the mean DDMA in different OSWS and mean OSWS in different DDMA, respectively. Then the orange dots are regressed by using the equation

$$y = ax^{-3} + bx^{-2} + cx^{-1} + \mathrm{d}. \tag{10}$$

For the left panel in Figure 4-1, $x$ and $y$ are OSWS and DDMA, respectively, and for the right panel, $x$ and $y$ are DDMA and OSWS. The coefficients $a$, $b$, $c$, and $\mathrm{d}$ of (10) in different signal incident angle are different. The relation between each coefficient and incident angle are regressed by using the equation

$$coe_{inc} = P_{coe}(inc)^2 + Q_{coe}(inc) + R_{coe}. \tag{11}$$

The original relation and regression results of the relation between coefficients and incident angle are shown in Figure 4-2. For retrieving, the input of the process are incident angle and DDMA. The coefficients of (10) can be calculated by using (11), and then wind speed can be calculated by using (10). The retrieval results of the data in Figure 4-1 are shown in red and yellow curves in the left and right panel, respectively. Tow OSWS are calculated by using two GMF. Combine two retrieval OSWS to obtain the final OSWS. The comparison between ECMWF OSWS and retrieval OSWS by using three DDMA calculated by using three different bin numbers of DDM are shown in Figure 4-3. The three comparisons are almost similar and the root mean square error (RMSE) is around 3m/s.

For MSS, the relation between MSS and NBRCS (CYGNSS, 2016) is

$$MSS = \frac{|\Re|^2}{\sigma_0} \tag{12}$$

where $\Re$ is Fresnel reflection coefficient, which is calculated by using incident angle of signal. However, NBRCS calculated of TRITON follows (9), which does not remove the effect of GPS satellite transmit power $P^T$ and GPS antenna gain $G^T$. In order to evaluate the effect of $P^T$ and $G^T$, the comparison between $\frac{|\Re|^2}{\sigma_0 P^T G^T}$ and ECMWF MSS is shown in Figure 4-4. In Figure 4-4, the green and yellow area, which contain most of data, show the linear relation. The data in green and yellow area is used for linear regression and the data used for regression and the regression result are shown in Figure 4-5. The regression result is used for the correction of NBRCS and then calculating MSS by using (12). The comparison between retrieval MSS and ECMWF MSS is shown in Figure 4-6.

For Hs, the GMF is used for retrieving. the comparison between ECMWF Hs and DDMA, and between DDMA and ECMWF Hs are shown in left and right panel of Figure 4-7, respectively. Compare Figure 4-7 with 4-1, DDMA is less sensitive to Hs than OSWS. Like GMF development of OSWS, the orange dots in the two panels are the mean DDMA in different Hs and mean Hs in different DDMA and are used for regression by using (10). The coefficients $a$, $b$, $c$, and $\mathrm{d}$ of (10) in different signal incident angle are used for regression by using (11). The Hs can be retrieved by using (10), which coefficients are calculated by using incident angle and (11). Like OSWS, Hs also can be retrieved by combining two GMF retrieval results. However, due to the insensitive of Hs to DDMA, the combination of two GMF retrieval results is not as well as OSWS. The comparison between retrieval and ECMWF Hs is shown in Figure 4-8. The gap at around 1m of retrieval Hs is caused by the insensitive of Hs to DDMA for two GMF retrieval results combination.

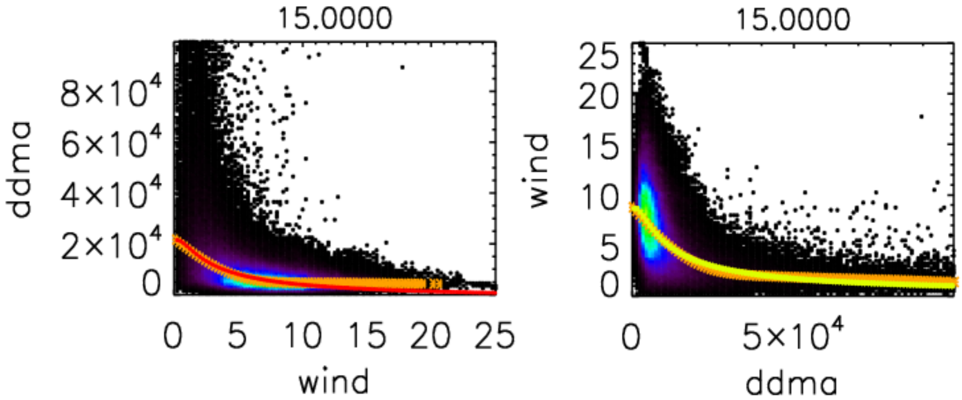


Figure 4-1 (left) Comparison between ECMWF OSWS and DDMA when signal incident angle around 15 degree. The orange dots are the mean DDMA in different OSWS and the red line is the regression line. (right) Comparison between DDMA and ECMWF OSWS when signal incident angle around 15 degree. The orange dots are the mean OSWS in different DDMA and yellow line is the regression line.

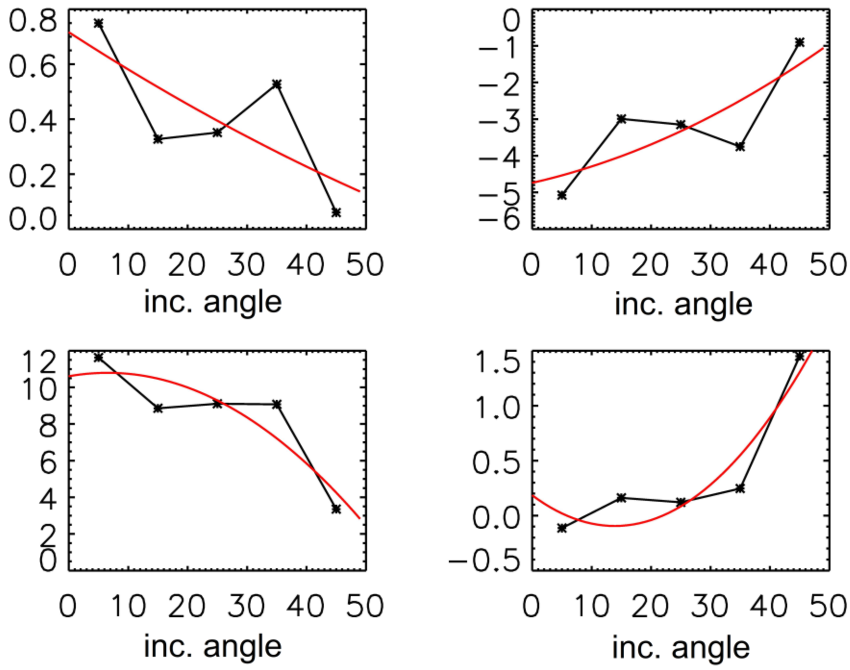


Figure 4-2 Equation coefficient variation in different incident angle. The black curves are the original value and red curves are the regression results. (left top) Variation of coefficient $a$ in (10). (right top) Variation of coefficient $b$ in (10). (left bottom) Variation of coefficient $c$ in (10). (right bottom) Variation of coefficient $d$ in (10).

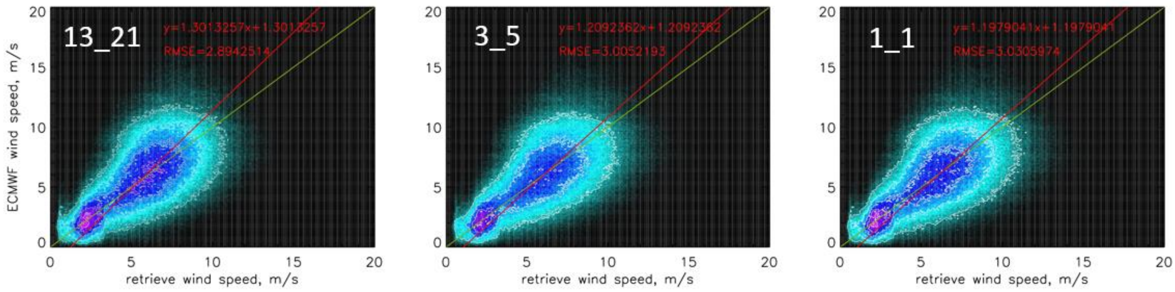


Figure 4-3 Comparisons between retrieval and ECMWF OSWS. Three retrieval OSWS are used for comparisons. (left) Retrieval OSWS by using $13 \times 21$ bins of DDM. (middle) Retrieval OSWS by using $3 \times 5$ bins of DDM. (right) Retrieval OSWS by using $1 \times 1$ bins of DDM.

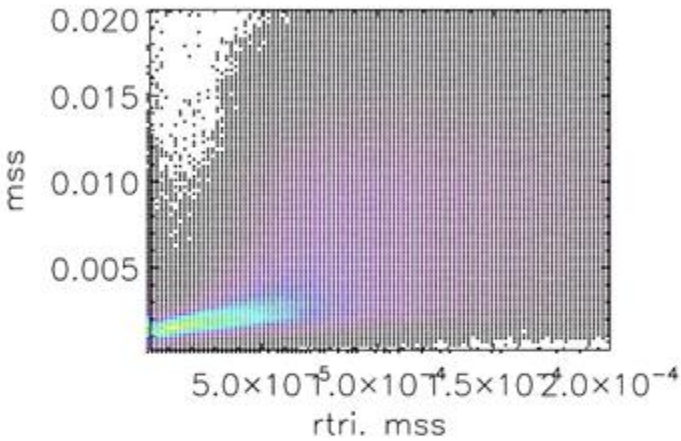


Figure 4-4 Comparison between NBRCS which calculated by (9), which does not remove the effect of GPS satellite transmit power and GPS antenna gain, and ECMWF MSS.

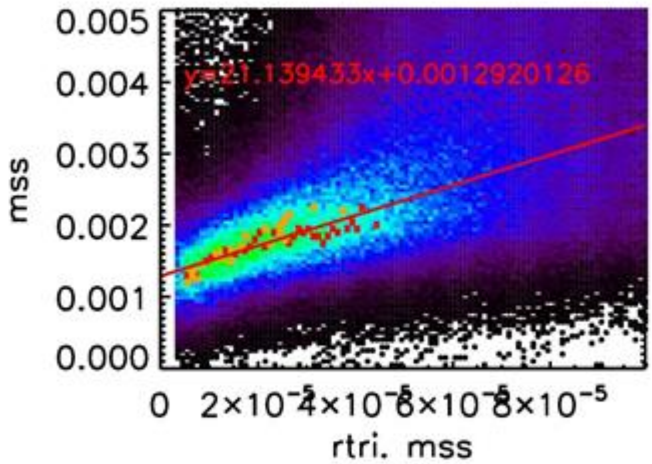


Figure 4-5 The orange and red dots in green area are used for linear regression.

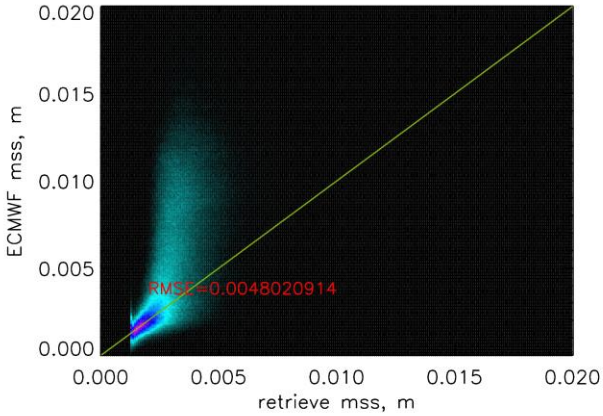


Figure 4-6 Comparison between retrieval and ECMWF MSS. The slope of green line is equal to 1.

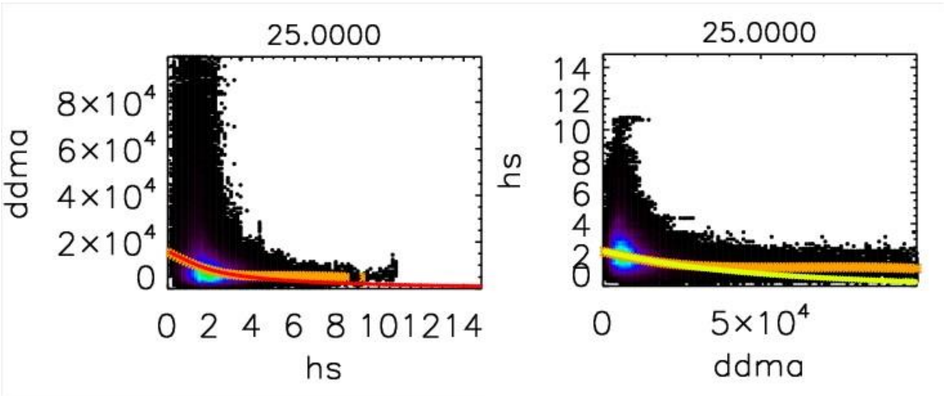


Figure 4-7 (left) Comparison between ECMWF Hs and DDMA when signal incident angle around 25 degree. The orange dots are the mean DDMA in different Hs and the red line is the regression line. (right) Comparison between DDMA and ECMWF Hs when signal incident angle around 25 degree. The orange dots are the mean Hs in different DDMA and yellow line is the regression line.

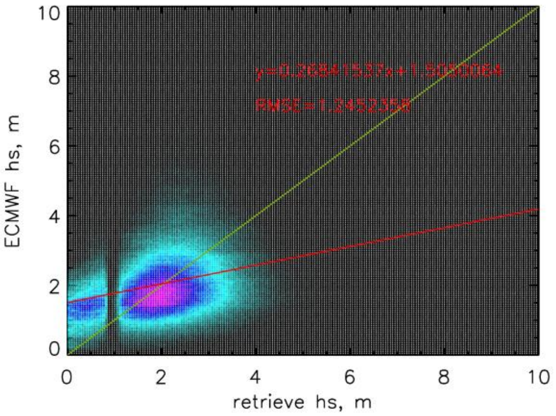


Figure 4-8 Comparison between retrieval and ECMWF Hs. The gap at around 1m retrieval Hs is caused by the insensitive of Hs to DDMA for two GMF retrieval results combination.

# 5 Reference


Zavorotny, V, Voronovich A (2000) Scattering of GPS signals from the ocean with wind remote sensing applications. IEEE Trans. Geosci. Remote Sens. 38(2): 951–964.

CYGNSS (2016) Algorithm Theoretical Basis Document Level 2 Mean-Square Slope Retrieval.

CYGNSS (2018) Algorithm Theoretical Basis Document Level 1B DDM Calibration.